Neurobiological correlates of attention and memory deficits following critical illness in early life

Raisa M. Schiller[1,2], MSc; Hanneke IJsselstijn[1], MD, PhD; Marlous J. Madderom[1], PhD; André B. Rietman[1,2], MSc; Marion Smits[4], MD, PhD; Arno F.J. van Heijst[3], MD, PhD; Dick Tibboel[1], MD, PhD; Tonya White[2,4] , MD, PhD; Ryan L. Muetzel[2], PhD

[1]Intensive Care and Department of Pediatric Surgery, Erasmus MC-Sophia Children's Hospital, Rotterdam, the Netherlands

[2]Department of Child and Adolescent Psychiatry/Psychology, Erasmus MC-Sophia Children's Hospital, Rotterdam, the Netherlands

[3]Department of Neonatology, Radboud University Medical Center, Nijmegen, the Netherlands

[4]Department of Radiology and Nuclear Medicine, Erasmus MC, Rotterdam, the Netherlands

Corresponding author: T. White

Department of Child and Adolescent Psychiatry/Psychology

Erasmus MC-Sophia Children's Hospital

3000 CB, Rotterdam, the Netherlands

Email: t.white@erasmusmc.nl

Telephone: +31 10 703 7072

No reprints will be ordered

Conflicts of Interest and Source of Funding: The authors declare that they have no conflict of interest. Financial support was provided by the Sophia Stichting Wetenschappelijk Onderzoek (SSWO): S14-21.

Key Words: extracorporeal membrane oxygenation; congenital diaphragmatic hernia; critical care outcomes; neuroimaging; memory; hippocampus

Word count: 2995

Abstract

Objective Survivors of critical illness in early life are at risk of long-term memory and attention impairments. However, their neurobiological substrates remain largely unknown.

Design A prospective follow-up study.

Setting Erasmus MC-Sophia Children's Hospital, Rotterdam, the Netherlands.

Patients Thirty-eight school-age (8-12 years) survivors of neonatal extracorporeal membrane oxygenation (ECMO) and/or congenital diaphragmatic hernia (CDH) with an IQ ≥ 80 and a below average score (z-score≤ -1.5) on one or more memory tests.

Interventions None.

Measurements and Main Results Intelligence, attention, memory, executive functioning and visuospatial processing were assessed and compared with reference data. White matter microstructure and hippocampal volume were assessed using Diffusion Tensor Imaging and structural MRI, respectively. Global fractional anisotropy(FA) was positively associated with selective attention (β=0.53, p=.030) and sustained attention (β=0.48, p=.018). Mean diffusivity(MD) in the left parahippocampal region of the cingulum (PHC) was negatively associated with visuospatial memory, both immediate (β=-0.48, p=.030) and delayed recall (β=-0.47, p=.030). MD in the PHC was negatively associated with verbal memory delayed recall (left:β=-0.52, p=.021; right:β=-0.52, p=.021). Hippocampal volume was positively associated with verbal memory delayed recall (left:β=0.44, p=.037; right:β=0.67, p=.012). ECMO treatment or ECMO type did not influence the structure-function relationships.

Conclusions Our findings indicate specific neurobiological correlates of attention and memory deficits in school-age survivors of neonatal ECMO and CDH. A better understanding of the neurobiology following critical illness, both in early and in adult life, may lead to earlier identification of patients at risk for impaired neuropsychological outcome with the use of neurobiological markers.

INTRODUCTION

The number of children admitted to neonatal intensive care units has increased over the last decade and medical improvements have led to higher survival rates(1). The long-term neurodevelopment following critical illness in early life is therefore, now more than ever, of major concern. Previous studies have shown that growing up after critical illness in early life, either due to prematurity, specific forms of cardiac anomalies or major congenital anomalies, is associated with neuropsychological deficits and school problems. Attention and memory domains have been reported in pre-adolescent and adolescent survivors, irrespective of underlying cause or birthweight(2-7). However, the neurobiological substrates of these impairments remain largely unknown.

A clearly delimited group of critical illness survivors are children treated with neonatal extracorporeal membrane oxygenation(ECMO) or congenital diaphragmatic hernia(CDH) treated without ECMO. Recently, we showed altered global white matter microstructure and specific alterations in limbic system regions in 11-year-old ECMO survivors(8). Hippocampal volume was positively associated with verbal memory(8). However, as only a limited cognitive assessment was available, specific aspects of neuropsychological outcome in relation to brain alterations have yet to be explored. This is of interest as, despite a generally average IQ, not only verbal but visuospatial memory and attention deficits have been shown following ECMO and CDH without ECMO(2, 5, 7).

The identification of impaired neurodevelopment currently relies solely on neuropsychological assessment. Understanding the neurobiological correlates of impaired outcome may lead to earlier identification of children at risk with the use of advanced neuroimaging techniques. In this study, we aimed to find neurobiological substrates of neuropsychological deficits in school-age (8-12 years) survivors of critical illness in early life by combining elaborate neuropsychological assessment with structural MRI and diffusion tensor imaging(DTI). We hypothesized that previously demonstrated brain alterations in neonatal ECMO survivors (i.e. global white matter microstructure, white matter microstructure in the cingulum bundle and parahippocampal region of the cingulum, and hippocampal volume(8)) would be specifically associated with memory and attention deficits. We expect our findings to aid in earlier identification of patients at risk of long-term cognitive deficits with the use of neurobiological markers.

MATERIALS AND METHODS

Population

Participants of an ongoing trial of working-memory training (NTR4571) at the Erasmus MC-Sophia Children's Hospital with usable neuroimaging data at baseline were included. Inclusion criteria for the trial were: school-age (8-12 years) children treated with ECMO or treated for CDH without ECMO in the first weeks of life at the Erasmus MC-Sophia Children's Hospital in Rotterdam or the Radboud University Medical Center in Nijmegen (the Netherlands), IQ ≥ 80 and memory impairment (*z*-score ≤ -1.5 on ≥1 memory tests(9)). Children who met the inclusion criteria underwent neuroimaging. ECMO treatment had been applied in case of reversible severe respiratory failure using the entry criteria by Stolar et al(10): oxygenation index>25 with 3-hour intervals, persistent low pH (<7.15) for 3-6 hours, and non-responding to changes in therapy. Entry criteria for ECMO did not change over time. Exclusion criteria were: psychopharmaceutical drugs (e.g. methylphenidate) and/or genetic syndromes known to affect neuropsychological functioning.

This study was performed in compliance with the Code of Ethics of the World Medical Association (Declaration of Helsinki) and approved by the Institutional Review Board (MEC-2014-001). All parents and children ≥12 years signed an informed consent prior to their inclusion in the study. The neuropsychological and neuroimaging data collected at baseline are presented in this study.

Neuropsychological assessment

Validated neuropsychological tests, with Dutch validated reference values, were assessed cognitive skills across four domains (brief test descriptions in Supplemental Digital Content 1):

1. *Intelligence:* Two-subtest(Block Design and Vocabulary) short-form(11) of the Wechsler Intelligence Scale for Children(WISC-III-NL)(12).
2. *Attention*:
    a. *Sustained attention*: Dot Cancellation Test(DCT)(13).
    b. *Selective attention*: Trail Making Test B(TMTB)(9), STROOP color-word test(Stroop)(9).
    c. *Processing speed*: Trail Making Test A(TMTA)(9).

3. *Memory:*
    a. *Working-memory:* subtest Digit Span of the WISC-III-NL(12), subtest Spatial Span of the Wechsler Nonverbal Scale of Ability(WNV)(14).
    b. *Verbal memory:* Rey Auditory Verbal Learning Test(RAVLT)(15).
    c. *Visuospatial memory:* Rey Complex Figure Test(RCFT)(16).
4. *Executive functioning:* Subtests Key Search and Modified Six Elements of the Behavioral Assessment of the Dysexecutive Syndrome(17).

Neuroimaging

All children first underwent a mock scanning session to become familiarized with the MR-environment(18). MRI data were acquired on a 3 Tesla GE MR-750 system using an 8-channel head coil(General Electric, Milwaukee, WI). A full description of the methods is provided in Supplemental Digital Content 2. After DTI data processing, the voxel-wise scalar maps fractional anisotropy(FA) and mean diffusivity(MD) were computed. FA indicates the degree of directionality of water diffusion and ranges from 0 to 1. MD is the rate of diffusion of water (hydrogen) averaged in all directions. The FSL plugin 'AutoPtx' for fully automated probabilistic fiber tractography was used to create subject-specific, probabilistic representations of multiple white matter bundles(19). Automated(20) and visual inspection of the data left 33 DTI datasets(87%) and 35 structural MRI datasets(92%) with usable image quality. All scans were reviewed by a board-certified neuroradiologist (M.S.), blinded for medical history and outcome. No serious clinically relevant abnormalities were reported. In one patient with a hemorrhagic infarct in the posterior middle cerebral artery as shown on neonatal cranial ultrasound, abnormalities (ulegyria) in this region were still visible on the long-term MRI scan. Sensitivity analyses were performed without this child's data. As the results did not change, the child was not excluded from the analyses.

Statistical analysis

Neuropsychological test scores were converted to z-scores (individual score minus the population mean divided by the population SD). Scores were inverted where appropriate so that higher scores always equated with better performance. Described in more detail in our previous study(8), global white matter microstructure was calculated using a weighted (by tract volume) average score of FA/MD of the association and limbic system fibers (uncinate, inferior fronto-occipital fasciculus, superior longitudinal fasciculus, inferior longitudinal fasciculus, cingulum bundle and parahippocampal part of cingulum(PHC)):

Formula 1:

$$\text{Global FA} = \frac{\sum_{i=1}^{6} FAtract_i Voltract_i}{\sum_{i=1}^{6} Voltract_i}$$

Where *i* denotes the tract, and *Vol* the volume of the tract. The same formula was used for global MD.

Our primary aim was to examine whether previously reported brain alterations in ECMO survivors (global white matter structure, FA in the cingulum bundle, MD in the PHC and hippocampal volume(8)) were associated with specific neuropsychological deficits in ECMO survivors and survivors of CDH treated without ECMO. Linear regression analyses were used to assess the associations between the brain regions of interest and neuropsychological outcome. Brain structures were analyzed in the left and right hemispheres separately. If a significant association existed between an individual white matter tract and neuropsychological outcome, global FA/MD was added to identify whether associations were specific to an individual white matter tract above and beyond a global effect. The False Discovery Rate(FDR) correction(21) was applied once for each set of analyses between the same neuropsychological task and white matter microstructure outcomes(i.e. once for every six tests). The same method was used for the analyses between neuropsychological outcome and hippocampal volume. In post-hoc analyses, we adjusted for IQ to assess whether the structure-function relationships were specific to that neuropsychological domain or driven by general intellectual functioning.

Next, we assessed whether ECMO treatment(yes/no) or type of ECMO treatment(venoarterial ECMO(VA-ECMO)/venovenous ECMO(VV-ECMO)) influenced the associations between the brain regions of interest and neuropsychological outcome using linear regression analyses(5, 22).

Finally, we determined if neuropsychological outcome was significantly different from the general population(mean z-score=0; SD=1) using one-sample t-tests, to inform us about the potential meaning of a significant structure-function relationship.

SPSS Statistics Version 22.0(Armonk, NY: IBM Corp.) was used for the statistical analyses. Normality tests were performed for all data and assumptions of ANCOVA were checked and met before analyses were conducted. No multicollinearity was found(variance inflation factors<2.5(23)). In all regression analyses, we adjusted for age at the time of assessment and gender(24). Total brain volume was included in the analyses with hippocampal volume(25). The standardized regression coefficient beta(β), uncorrected(p_{uncor}) and FDR-corrected *p*-values were reported. Effect sizes were calculated using partial eta squared(h_p^2) and interpreted according to Cohen's guidelines (0.01=small, 0.06=medium, 0.14=large)(26). Results were considered statistically significant at FDR-corrected $p<.05$.

RESULTS

Study population

Thirty-eight children participated (15 girls, 23 boys) with a mean age(SD) of 9.7(1.5) years. Twenty-six children (68%) had been treated with ECMO (MAS=18; CDH=2; Other=6) and 12 CDH patients (32%) had not required ECMO. Seventeen ECMO patients (65%) had undergone VA-cannulation and nine (35%) VV-ECMO. Patient characteristics retrieved from medical records are reported in Table 1.

White matter microstructure and neuropsychological outcome

Lower global FA was associated with worse selective attention, β=0.45, p=.036, h_p^2=0.24, and sustained attention, β=0.48, p=.018, h_p^2=0.23(Table 2). Lower FA in the right cingulum bundle was associated with worse sustained attention, β=0.46, p=.018, h_p^2=0.24, whereas the association with FA in the left cingulum bundle disappeared after correcting for multiple testing, β=0.40, p=.046, h_p^2=0.26. These findings were no longer significant when global FA was added(Table 2).

No associations were found between global MD and any of the neuropsychological tests(Table 2). Higher MD in the left PHC was associated with worse visuospatial memory immediate recall, β= -0.48, p=.030, h_p^2=0.24, and delayed recall, β= -0.47, p=.030, h_p^2=0.24. MD in both the left and right PHC were also negatively associated with verbal memory delayed recall (left: β= -0.52, p=.021, h_p^2=0.23; right: β= -0.52, p=.021, h_p^2=0.26)(Table 2, Figure 1).

IQ did not affect the associations between white matter microstructure and neuropsychological outcome.

Hippocampal volume and neuropsychological outcome

Smaller hippocampal volumes in the left and right hemispheres were associated with lower scores on verbal memory delayed recall (left: β=0.44, p=.037, h_p^2=0.16; right: β=0.67, p=.012, h_p^2=0.14)(Table 3, Figure 1). IQ did not affect these associations.

Treatment characteristics and neurodevelopmental outcome

The significant associations found between neuropsychological outcome and the brain were the same in ECMO and non-ECMO patients, and VA-ECMO and VV-ECMO patients(Supplemental Digital Content 3).

Neuropsychological functioning compared to the norm population

Participants had an average IQ but scored significantly lower on all verbal and visuospatial memory tasks (immediate recall, delayed recall and recognition). Participants also had significantly lower sustained attention than the reference population(Table 4).

DISCUSSION

The aim of this study was to identify neurobiological substrates of long-term impaired neuropsychological outcome following critical illness in early life. In CDH survivors treated with and without ECMO and in survivors of ECMO treatment following other diagnoses, specific associations were found between attention and memory deficits and global white matter microstructure and regions of the limbic system. These results – that were irrespective of ECMO or conservative ventilator management – provide more insight in the underlying neurobiology of long-term outcome following critical illness in early life. Furthermore, our findings were irrespective of general IQ. This supports a 'growing into deficit' phenomenon in these patients, where subtle brain injuries acquired at a young age become functionally evident when higher cognitive functioning is required at a later age.

The PHC and hippocampus are part of the limbic system, one of the main brain networks involved in memory. The PHC is bidirectionally connected to the hippocampus and forms a larger memory circuit together with cortical structures(27). While the hippocampus is viewed as the main hub for memory, its connections are highly important for intact functioning of various memory types (27, 28). In line with this, our findings showed higher MD, suggestive of decreased integrity in axonal membranes, packing, or myelin(29), in the PHC to be associated with lower visuospatial and verbal memory. Further, smaller hippocampal volume was associated with impaired verbal memory. Interestingly, studies on other types of critical illness in early life have demonstrated similar structure-function relationships. Hippocampal alterations and related verbal memory impairments were previously found by our group in a different cohort of neonatal ECMO survivors, but also by others in survivors of neonatal hypoxia and in patients with severe forms of congenital heart disease(3, 8, 30). In preterms, infant hippocampal volume was negatively associated with school-age verbal memory, and white matter volume in the PHC with non-verbal memory (31, 32).

The present study further showed that lower global FA was related to poorer attention. Lower FA can be interpreted as reduced coherence of white matter fibers(29). Global white matter abnormalities have been associated with lower attention in preterms as well(33). Although we also found a significant association between lower FA in the cingulum bundle and worse sustained attention, this

association disappeared when global FA was added. These findings support the notion of more widespread white matter network alterations underlying attention impairments(34).

In our study, the majority of significant structure-function relationships were found in the left and right hemispheres, although associations with FA in the left cingulum bundle disappeared after multiple testing correction. The associations with visuospatial memory were found only in the left PHC. Predominantly left hemispheric alterations have been suggested to be due to right internal jugular vein cannulation in neonatal ECMO patients(35). However, our results did not show an effect of ECMO. CDH survivors treated without ECMO showed structure-function relationships similar to ECMO-treated patients. Also, no differences were found between VA- and VV-ECMO treated patients. However, these findings should be interpreted with caution due to the small sample size. Furthermore, previous findings have shown more brain abnormalities in VA-ECMO-treated patients compared to VV-treated patients, but associations with neuropsychological outcome were not studied(22). Future studies with larger sample sizes, also including near-ECMO patients, are needed to further delineate the effects of treatment or diagnosis on neurodevelopment following critical illness.

Although further research is needed, our results suggest similar neuropsychological deficits and structure-function relationships in CDH survivors treated with and without ECMO and ECMO survivors following other diagnoses. This may suggest potentially similar neurodevelopmental mechanisms following various types of critical illness in early life(3, 30-32). The brain matures in a nonlinear fashion from childhood into adulthood, indicating that the timing of microstructural changes differs per brain region(24, 36). Consequently, the timing of injuries is likely to have specific effects on brain development(37). As the limbic system undergoes rapid development in the third trimester and neonatal period, these structures may be particularly vulnerable in critically ill newborns, born prematurely and at term(38, 39). Furthermore, the hippocampus is sensitive to both internal and external influences. Hypoxic-ischemic injury and (chronic) stress have been associated with hippocampal alterations in term and preterm infants(40, 41). White matter limbic system fibers, such as the PHC and cingulum bundle, may be more vulnerable to these types of injuries because of their connections with the hippocampus and their periventricular location(37). Interestingly, similar long-term cognitive impairments were reported in adult patients after treatment at intensive care units (ICU)(42). Although newborns are likely

to be at higher risk of limbic system alterations due to its rapid development during this time, hippocampal vulnerability has been shown in the adult brain as well but needs further exploration in adult ICU survivors(43).

While this study contributes to the limited research on the neurobiology of neuropsychological outcome following critical illness, there are some limitations. First, our comparisons between ECMO and non-ECMO, and VA- and VV-ECMO treated patients should be interpreted with caution as the small sample size limits the interpretability of the regression analyses. Second, we did not have a (healthy) control group to compare our neuroimaging data with. Due to major differences in scanner hardware and software, we could not compare our data to data obtained elsewhere. We did however have normative data of the neuropsychological tests. Since we were primarily interested in finding potential neurobiological substrates of impaired outcome following critical illness, we were still able to adequately address these questions. Third, our sample includes only children with a below average score on one or more memory tests and an IQ of 80 or above. However, since previous studies have shown that the majority of ECMO and CDH survivors have average intelligence but an increased likelihood of attention and memory impairments(2, 5, 7), we feel this sample is representative of critical illness survivors and suits the aim of this study. Nonetheless, future studies should explore how below average IQ affects the structure-function relationships.

CONCLUSIONS

We showed that regions of the limbic system and global white matter microstructure were specifically related to impaired neuropsychological outcome in school-age survivors of CDH treated with and without ECMO and in ECMO survivors following other diagnoses. Our findings may lead to earlier identification of those at risk of neurodevelopmental impairment with the use of neurobiological markers, such as low hippocampal volume. Also, a better understanding of the neurobiology will contribute to a more critical appraisal of potential intervention modalities. As similar neurodevelopmental outcomes have been found in survivors of various causes of critical illness, future research should assess neurodevelopment longitudinally across different patient groups using both neuroimaging and neuropsychological assessment and compare outcomes to age-matched healthy controls.

ACKNOWLEGDMENTS

This study was supported by the Sophia Stichting Wetenschappelijk Onderzoek (SSWO): S14-21.

REFERENCES

1. Harrison W, Goodman D. Epidemiologic Trends in Neonatal Intensive Care, 2007-2012. JAMA Pediatr 2015;169(9):855-862.

2. Schiller RM, Madderom MJ, Reuser JJCM, et al. Neuropsychological follow-up after neonatal ECMO. Pediatrics 2016;138(5) :e20161313.

3. Cooper JM, Gadian DG, Jentschke S, et al. Neonatal hypoxia, hippocampal atrophy, and memory impairment: evidence of a causal sequence. Cereb Cortex 2015;25(6):1469-1476.

4. Beauchamp MH, Thompson DK, Howard K, et al. Preterm infant hippocampal volumes correlate with later working memory deficits. Brain 2008;131(Pt 11):2986-2994.

5. Madderom MJ, Toussaint L, van der Cammen-van Zijp MH, et al. Congenital diaphragmatic hernia with(out) ECMO: impaired development at 8 years. Arch Dis Child Fetal Neonatal Ed 2013;98(4):F316-322.

6. Jerrell JM, Shuler CO, Tripathi A, et al. Long-Term Neurodevelopmental Outcomes in Children and Adolescents With Congenital Heart Disease. Prim Care Companion CNS Disord 2015;17(5).

7. Madderom MJ, Schiller RM, Gischler SJ, et al. Growing Up After Critical Illness: Verbal, Visual-Spatial, and Working Memory Problems in Neonatal Extracorporeal Membrane Oxygenation Survivors. Crit Care Med 2016;44(6):1182-1190.

8. Schiller RM, van den Bosch GE, Muetzel RL, et al. Neonatal critical illness and development: white matter and hippocampus alterations in school-age neonatal extracorporeal membrane oxygenation survivors. Dev Med Child Neurol 2017;59(3):304-310.

9. Lezak MD, Howieson DB, Loring DW. Neuropsychological assessment, 4th ed. Oxford: Oxford University Press; 2004.

10. Stolar CJ, Snedecor SM, Bartlett RH. Extracorporeal membrane oxygenation and neonatal respiratory failure: experience from the extracorporeal life support organization. J Pediatr Surg 1991;26(5):563-571.

11. Kaufman AS, Kaufman JC, Balgopal R, et al. Comparison of three WISC-III short forms: Weighing psychometric, clinical, and practical factors. J Clin Child Psychol 1996;25(1):97-105.

12. Kort W, Compaan EL. WISC NL III. Handleiding: NIP Dienstencentrum 1999.

13. Vos P. Bourdon-Vos. Handleiding (manual dot cancellation test). Lisse: Swets en Zeitlinger; 1992.

14. Wechsler D, Naglieri JA. Wechsler Nonverbal Scale of Ability San Antonio, TX: Pearson; 2006.

15. van den Burg W, Kingma A. Performance of 225 Dutch school children on Rey's Auditory Verbal Learning Test (AVLT): parallel test-retest reliabilities with an interval of 3 months and normative data. Arch Clin Neuropsychol 1999;14(6):545-559.

16. Watanabe K, Ogino T, Nakano K, et al. The Rey-Osterrieth Complex Figure as a measure of executive function in childhood. Brain Dev 2005;27(8):564-569.

17. Emslie H, Wilson FC, Burden V, et al. Behavioral assessment of the dysexecutive syndrome for children (BADS-C), Dutch version. Amsterdam Harcourt; 2006.

18. White T, El Marroun H, Nijs I, et al. Pediatric population-based neuroimaging and the Generation R Study: the intersection of developmental neuroscience and epidemiology. Eur J Epidemiol 2013;28(1):99-111.

19. de Groot M, Ikram MA, Akoudad S, et al. Tract-specific white matter degeneration in aging: the Rotterdam Study. Alzheimers Dement 2015;11(3):321-330.

20. Muetzel RL, Mous SE, van der Ende J, et al. White matter integrity and cognitive performance in school-age children: A population-based neuroimaging study. Neuroimage 2015;119:119-128.

21. Benjamini Y, Hochberg Y. Controlling the False Discovery Rate - a Practical and Powerful Approach to Multiple Testing. J Roy Stat Soc B Met 1995;57(1):289-300.

22. Rollins MD, Yoder BA, Moore KR, et al. Utility of neuroradiographic imaging in predicting outcomes after neonatal extracorporeal membrane oxygenation. J Pediatr Surg 2012;47(1):76-80.

23. Allison P. Logistic regression using the SAS system: theory and application. . New York: SAS Institute; 1999.

24. Lebel C, Walker L, Leemans A, et al. Microstructural maturation of the human brain from childhood to adulthood. Neuroimage 2008;40(3):1044-1055.

25. Lin M, Fwu PT, Buss C, et al. Developmental changes in hippocampal shape among preadolescent children. Int J Dev Neurosci 2013;31(7):473-481.

26. Cohen J. Statistical power analysis for the behavioral sciences, 2nd ed Hilsdale, NJ: Lawrence Earlbaum Associates; 1988.

27. Eichenbaum H. How does the brain organize memories? Science 1997;277(5324):330-332.

28. Nosarti C, Froudist-Walsh S. Alterations in development of hippocampal and cortical memory mechanisms following very preterm birth. Dev Med Child Neurol 2016;58 Suppl 4:35-45.

29. Beaulieu C. The basis of anisotropic water diffusion in the nervous system - a technical review. NMR Biomed 2002;15(7-8):435-455.

30. Miller SP, McQuillen PS, Hamrick S, et al. Abnormal brain development in newborns with congenital heart disease. N Engl J Med 2007;357(19):1928-1938.

31. Thompson DK, Adamson C, Roberts G, et al. Hippocampal shape variations at term equivalent age in very preterm infants compared with term controls: perinatal predictors and functional significance at age 7. Neuroimage 2013;70:278-287.

32. Nosarti C, Nam KW, Walshe M, et al. Preterm birth and structural brain alterations in early adulthood. Neuroimage Clin 2014;6:180-191.

33. Woodward LJ, Clark CA, Pritchard VE, et al. Neonatal white matter abnormalities predict global executive function impairment in children born very preterm. Dev Neuropsychol 2011;36(1):22-41.

34. Petersen SE, Posner MI. The attention system of the human brain: 20 years after. Annu Rev Neurosci 2012;35:73-89.

35. Raets MM, Dudink J, Ijsselstijn H, et al. Brain injury associated with neonatal extracorporeal membrane oxygenation in the Netherlands: a nationwide evaluation spanning two decades. Pediatr Crit Care Med 2013;14(9):884-892.

36. Paus T, Zijdenbos A, Worsley K, et al. Structural maturation of neural pathways in children and adolescents: in vivo study. Science 1999;283(5409):1908-1911.

37. Back SA, Riddle A, McClure MM. Maturation-dependent vulnerability of perinatal white matter in premature birth. Stroke 2007;38(2 Suppl):724-730.

38. Dubois J, Dehaene-Lambertz G, Kulikova S, et al. The early development of brain white matter: a review of imaging studies in fetuses, newborns and infants. Neuroscience 2014;276:48-71.

39. Huang H, Zhang J, Wakana S, et al. White and gray matter development in human fetal, newborn and pediatric brains. Neuroimage 2006;33(1):27-38.

40. Kuchna I. Quantitative studies of human newborns' hippocampal pyramidal cells after perinatal hypoxia. Folia Neuropathol 1994;32(1):9-16.

41. Peng NH, Bachman J, Jenkins R, et al. Relationships between environmental stressors and stress biobehavioral responses of preterm infants in NICU. J Perinat Neonatal Nurs 2009;23(4):363-371.

42. Pandharipande PP, Girard TD, Jackson JC, et al. Long-term cognitive impairment after critical illness. N Engl J Med 2013;369(14):1306-1316.

43. Bartsch T, Wulff P. The hippocampus in aging and disease: From plasticity to vulnerability. Neuroscience 2015;309:1-16.

FIGURE LEGENDS

Figure 1.

Yellow and orange colors indicate a positive association and blue colors indicate a negative association between brain regions and neuropsychological outcome. a) Parasaggital and coronal views of the left and right hemispheres showing the left and right hippocampal volumes(1) and the left and right parahippocampal regions of the cingulum(2). b) Showing the associations between verbal memory delayed recall and mean diffusivity in the parahippocampal region of the cingulum and the hippocampal volume in both hemispheres. c) Showing the associations between visuospatial memory immediate and delayed recall and mean diffusivity in the parahippocampal region of the cingulum in both hemispheres. *Indicates a significant association at $p < .05$. Abbreviations: PHC, parahippocampal region of the cingulum.

SUPPLEMENTAL DIGITAL CONTENT

Supplemental Digital Content 1. Descriptions of the neuropsychological tests.

Brief descriptions of the neuropsychological tests used.

Supplemental Digital Content 2. Neuroimaging methods.

A full description of the structural MRI and diffusion tensor imaging methods used.

Supplemental Digital Content 3. Influence of ECMO treatment and type of ECMO on structure-function relationships.

Table showing the results of linear regression analyses assessing differences between patients treated with ECMO and without ECMO in the significant structure-function relationships, and differences between patients treated with venoarterial and venovenous ECMO.

Table 1. Patient characteristics

Patient characteristics	All (n = 38)	ECMO (n = 26)	CDH non-ECMO (n = 12)
Age at assessment (years)	9.7 ± 1.5	9.6 ± 1.7	10.0 ± 1.2
Gestational age (weeks)	40.0 ± 0.3	41 ± 1.4	39 ± 2.3
Birth weight (grams)	3410 (3205-3790)	3595 (3296-3822)	3133 (2414-3423)
Male	23 (61%)	14 (54%)	9 (75%)
Dutch ethnicity	32 (84%)	20 (77%)	12 (100%)
Days of mechanical ventilation	10 (8-16)	11 (9-17)	9 (6-16)
Neonatal brain abnormalities[1]	3 (9%)	3 (13%)	0
Inborn	7 (18%)	1 (4%)	6 (50%)
Diagnosis			
MAS		18 (69%)	
CDH		2 (8%)	12 (100%)
Other[2]		6 (23%)	
Age start ECMO (days)		2 (1-3)	
Duration of ECMO (hours)		114 (89-181)	
Type of ECMO			
VA		16 (61%)	
VV		9 (35%)	
VV to VA conversion		1 (4%)	

Data are expressed as mean ± SD, median (IQR) or number (percentage), as appropriate.

1 Abnormalities seen on cranial ultrasound or MRI in neonatal period: hemorrhagic infarct in the posterior middle cerebral artery (n= 1), bilateral thalamic lesions (n=2).

2 Other diagnoses are PPHN (n=3), respiratory insufficiency due to respiratory syncytial virus (n=2), monoventricular heart with transposition of the great vessels (n=1).

Abbreviations: ECMO, extracorporeal membrane oxygenation; CDH, congenital diaphragmatic hernia; MAS, meconium aspiration syndrome; PPHN, persistent pulmonary hypertension of the newborn.

Table 2. White matter microstructure and neuropsychological outcome.

Neuropsychological test, n = 33	Global FA	FA CB left	FA CB right	Global MD	MD PHC left	MD PHC right
Intelligence						
WISC-III-NL	β = 0.16, $p_{uncor.}$= .426, p = .680	β = 0.08, $p_{uncor.}$ = .680, p = .680	β = 0.26, $p_{uncor.}$= .158, p = .474	β = -0.13, $p_{uncor.}$= .564, p = .680	β = 0.09, $p_{uncor.}$= .642, p = .680	β = 0.27, $p_{uncor.}$= .146, p = .474
Attention						
TMT A	β = 0.20, $p_{uncor.}$= .324, p = .648	β = 0.15, $p_{uncor.}$= .468, p = .702	β = 0.23, $p_{uncor.}$= .227, p = .648	β = 0.12, $p_{uncor.}$= .587, p = .704	β = -0.00, $p_{uncor.}$= .983, p = .983	β = 0.32, $p_{uncor.}$= .083, p = .498
TMT B	**β = 0.53, $p_{uncor.}$= .005, p = .030**	β = 0.22, $p_{uncor.}$= .277, p = .397	β = 0.36, $p_{uncor.}$= .045, p = .135	β = -0.35, $p_{uncor.}$= .103, p = .206	β = -0.19, $p_{uncor.}$= .331, p = .397	β = 0.13, $p_{uncor.}$= .489, p = .489
Stroop interference	β = -0.14, $p_{uncor.}$= .450, p = .675	β = -0.32, $p_{uncor.}$= .064, p = .384	β = -0.01, $p_{uncor.}$= .966, p = .969	β = 0.24, $p_{uncor.}$= .223, p = .460	β = 0.01, $p_{uncor.}$= .969, p = .969	β = 0.20, $p_{uncor.}$= .230, p = .460
DCT	**β = 0.48, $p_{uncor.}$= .006, p = .018**	β = 0.40, $p_{uncor.}$= .023, p = .046*	**β = 0.46, $p_{uncor.}$= .004, p = .018***	β = -0.35, $p_{uncor.}$= .069, p = .104	β = -0.29, $p_{uncor.}$= .110, p = .132	β = -0.08, $p_{uncor.}$= .620, p = .620
Verbal memory						
Digit span	β = 0.08, $p_{uncor.}$= .685, p = .685	β = 0.14, $p_{uncor.}$= .484, p = .581	β = 0.26, $p_{uncor.}$= .158, p = .358	β = 0.25, $p_{uncor.}$= .257, p = .386	β = 0.32, $p_{uncor.}$= .108, p = .358	β = 0.25, $p_{uncor.}$= .179, p = .358
RAVLT immediate	β = 0.32, $p_{uncor.}$= .111, p = .333	β = 0.22, $p_{uncor.}$= .274, p = .411	β = 0.09, $p_{uncor.}$= .631, p = .631	β = -0.21, $p_{uncor.}$= .350, p = .420	β = -0.41, $p_{uncor.}$= .036, p = .216	β = -0.25, $p_{uncor.}$= .192, p = .384
RAVLT delayed	β = 0.21, $p_{uncor.}$= .313, p = .470	β = 0.04, $p_{uncor.}$= .851, p = .851	β = -0.04, $p_{uncor.}$= .831, p = .851	β = -0.24, $p_{uncor.}$= .284, p = .670	**β = -0.52, $p_{uncor.}$= .007, p = .021**	**β = -0.52, $p_{uncor.}$= .004, p = .021**
RAVLT recognition	β = 0.15, $p_{uncor.}$= .464, p = .873	β = 0.16, $p_{uncor.}$= .437, p = .873	β = 0.03, $p_{uncor.}$= .878, p = .893	β = 0.03, $p_{uncor.}$= .893, p = .893	β = -0.12, $p_{uncor.}$= .582, p = .873	β = -0.24, $p_{uncor.}$= .209, p = .873
Visuospatial memory						
Spatial Span	β = 0.02, $p_{uncor.}$ = .913, p = .945	β = 0.04, $p_{uncor.}$= .848, p = .945	β = -0.10, $p_{uncor.}$= .945, p = .945	β = -0.02, $p_{uncor.}$= .913, p = .945	β = 0.13, $p_{uncor.}$= .519, p = .945	β = 0.25, $p_{uncor.}$= .164, p = .945
RCFT immediate	β = 0.18, $p_{uncor.}$= .320, p = .480	β = -0.05, $p_{uncor.}$= .778, p = .934	β = -0.01, $p_{uncor.}$= .963, p = .963	β = -0.30, $p_{uncor.}$= .131, p = .393	**β = -0.48, $p_{uncor.}$= .005, p = .030**	β = -0.20, $p_{uncor.}$= .243, p = .480
RCFT delayed	β = 0.23, $p_{uncor.}$= .203, p = .406	β = -0.02, $p_{uncor.}$= .932, p = .932	β = -0.04, $p_{uncor.}$= .806, p = .932	β = -0.29, $p_{uncor.}$= .130, p = .390	**β = -0.47, $p_{uncor.}$= .005, p = .030**	β = -0.16, $p_{uncor.}$= .324, p = .486
RCFT recognition	β = 0.36, $p_{uncor.}$= .056, p = .112	β = 0.18, $p_{uncor.}$= .346, p = .519	β = 0.05, $p_{uncor.}$= .765, p = .820	β = -0.44, $p_{uncor.}$= .028, p = .084	β = -0.42, $p_{uncor.}$= .022, p = .084*	β = 0.04, $p_{uncor.}$= .820, p = .820
Executive functioning						
Key Search	β = -0.04, $p_{uncor.}$= .808, p = .808	β = -0.26, $p_{uncor.}$= .138, p = .549	β = -0.12, $p_{uncor.}$= .461, p = .692	β = 0.25, $p_{uncor.}$= .183, p = .549	β = 0.06, $p_{uncor.}$= .752, p = .808	β = 0.15, $p_{uncor.}$= .357, p = .692
Modified six elements	β = 0.20, $p_{uncor.}$= .333, p = .635	β = 0.15, $p_{uncor.}$= .451, p = .635	β = 0.13, $p_{uncor.}$= .529, p = .635	β = -0.09, $p_{uncor.}$= .686, p = .686	β = -0.26, $p_{uncor.}$= .200, p = .600	β = -0.26, $p_{uncor.}$= .200, p = .600
Visuospatial processing						
RCFT copy	β = 0.24, $p_{uncor.}$ = .248, p = .743	β = 0.13, $p_{uncor.}$= .522, p = .743	β = 0.11, $p_{uncor.}$= .549, p = .743	β = -0.29, $p_{uncor.}$= .188, p = .743	β = 0.01, $p_{uncor.}$= .953, p = .953	β = 0.10, $p_{uncor.}$= .619, p = .743

Results of linear regression analyses assessing associations between our brain regions of interest[8] and neuropsychological outcome, adjusted for gender and age at assessment. *puncor.* gives the uncorrected *p*-value. ***P*** < .05 is considered statistically significant after correcting for multiple testing using the false discovery rate correction. *No longer significant when global measure of microstructure was added to the model.

Abbreviations: FA, fractional anisotropy; CB, cingulum bundle; MD, mean diffusivity; PHC, parahippocampal region of the cingulum; WISC-III-NL, Wechsler Intelligence Scale for Children Dutch version; TMT, Trail Making Test; DCT, Dot Cancellation Test; RAVLT, Rey Auditory Verbal Learning Test; RCFT, Rey Complex Figure Test..

Table 3. Hippocampal volume and neuropsychological outcome

Neuropsychological test n= 38	Hippocampal volume, left	Hippocampal volume, right
Intelligence		
WISC-III-NL	β = 0.12, $p_{uncor.}$= .583, p = .868	β = 0.04, $p_{uncor.}$= .868, p = .868
Attention		
TMT A	β = -0.04, $p_{uncor.}$= .862, p = .862	β = -0.08, $p_{uncor.}$= .799, p = .862
TMT B	β = -0.20, $p_{uncor.}$= .364, p = .470	β = -0.19, $p_{uncor.}$= .470, p = .470
Stroop interference	β = 0.10, $p_{uncor.}$= .645, p = .900	β = 0.03, $p_{uncor.}$= .900, p = .900
DCT	β = 0.07, $p_{uncor.}$= .716, p = .950	β = -0.02, $p_{uncor.}$= .950, p = .950
Verbal Memory		
Digit span	β = -0.10, $p_{uncor.}$= .624, p = .624	β = -0.42, $p_{uncor.}$= .073, p = .146
RAVLT immediate	β = 0.40, $p_{uncor.}$= .057, p = .114	β = 0.36, $p_{uncor.}$= .148, p = .148
RAVLT delayed	**β = 0.44, $p_{uncor.}$= .037, p = .037**	**β = 0.67, $p_{uncor.}$= .006, p = .012**
RAVLT recognition	β = 0.27, $p_{uncor.}$= .238, p = .238	β = 0.40, $p_{uncor.}$= .144, p = .238
Visuospatial memory		
Spatial Span	β = 0.04, $p_{uncor.}$= .842, p = .920	β = -0.03, $p_{uncor.}$= .920, p = .920
RCFT immediate	β = 0.30, $p_{uncor.}$= .133, p = .133	β = 0.39, $p_{uncor.}$= .103, p = .133
RCFT delayed	β = 0.22, $p_{uncor.}$= .264, p = .290	β = 0.24, $p_{uncor.}$= .290, p = .290
RCFT recognition	β = -0.05, $p_{uncor.}$= .825, p = .825	β = -0.08, $p_{uncor.}$= .748, p = .825
Executive Functioning		
Key Search	β = 0.17, $p_{uncor.}$= .358, p = .716	β = 0.04, $p_{uncor.}$= .859, p = .859
Modified six elements	β = 0.22, $p_{uncor.}$= .328, p = .328	β = 0.49, $p_{uncor.}$= .074, p = .074
Visual spatial processing		
RCFT copy	β = -0.00, $p_{uncor.}$= .987, p = .987	β = -0.04, $p_{uncor.}$= .889, p = .987

Results of linear regression analyses assessing associations between neuropsychological outcome and hippocampal volume in the left and right hemispheres. *Puncor*. gives the uncorrected *p*-value. ***P*** < .05 is considered statistically significant after correcting for multiple testing using the false discovery rate correction. Abbreviations: WISC-III-NL, Wechsler Intelligence Scale for Children Dutch version; TMT, Trail Making Test; DCT, Dot Cancellation Test; RAVLT, Rey Auditory Verbal Learning Test; RCFT, Rey Complex Figure Test.

Table 4. Overview of neuropsychological assessment outcome		
Neuropsychological test	All (n = 38)	*P* value[1]
Intelligence		
WISC-III-NL[2]	100 (12)	.968
Attention		
TMT A	-0.33 (0.95)	.057
TMT B	-0.03 (1.18)	.954
Stroop interference	-0.31 (1.00)	.063
DCT	**-1.13 (2.01)**	**.001**
Memory		
WISC-III-NL Digit span	0.21 (1.02)	.219
WNV Spatial Span	0.17 (1.02)	.336
RAVLT immediate	**-1.58 (1.10)**	**.000**
RAVLT delayed	**-1.90 (1.19)**	**.000**
RAVLT recognition	**-1.19 (1.59)**	**.000**
RCFT immediate	**-1.65 (0.97)**	**.000**
RCFT delayed	**-1.65 (1.07)**	**.000**
RCFT recognition	**-0.63 (1.45)**	**.007**
Executive functioning		
Key Search	0.01 (1.20)	.669
Modified six elements	-0.08 (0.99)	.652
Visual spatial processing		
RCFT copy	0.14 (0.68)	.205

Data are expressed as mean z-score ± SD. ***P*** **< .05** is considered statistically significant.

1P value of the one-sample t-test assessing the difference between the average z-score of the participants and the general population z-score ($\mu = 0$).

2IQ was based on a short-form of the WISC-III-NL using two subtests, Vocabulary and Block Design.[11] Abbreviations: WISC-III-NL, Wechsler Intelligence Scale for Children Dutch version; TMT, Trail Making Test; DCT, Dot Cancellation Test; RAVLT, Rey Auditory Verbal Learning Test; RCFT, Rey Complex Figure Test.

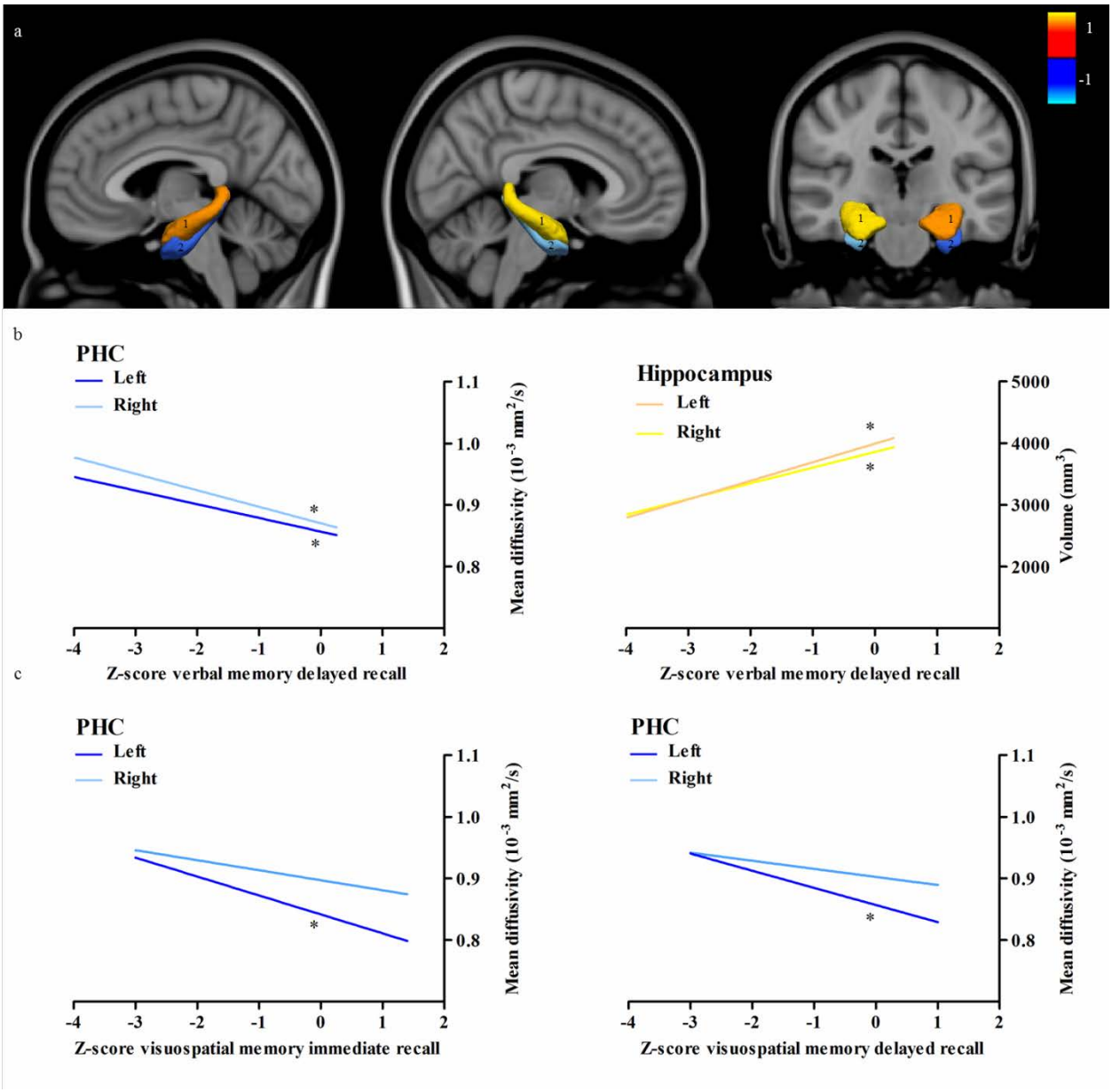
a
1
-1
b
PHC
Left
Right
Mean diffusivity (10^{-3} mm^2/s)
Z-score verbal memory delayed recall
Hippocampus
Left
Right
Volume (mm^3)
Z-score verbal memory delayed recall
c
PHC
Left
Right
Mean diffusivity (10^{-3} mm^2/s)
Z-score visuospatial memory immediate recall
PHC
Left
Right
Mean diffusivity (10^{-3} mm^2/s)
Z-score visuospatial memory delayed recall

Supplemental Digital Content 1. Descriptions of the neuropsychological tests.

Intelligence

Wechsler Intelligence Scale for Children (WISC-III-NL)

A short-form with two subtests, Block Design and Vocabulary, of the WISC-III-NL were used to assess general intelligence.(1) The WISC-III-NL has been shown to have good reliability and validity.(2) A normalized population mean of 100 with a standard deviation of 15 is used.(2)

Attention

Dot Cancellation Test

This paper-and-pencil test measures sustained attention and concentration in terms of speed. It consists of a paper on which figures made of three, four or five dots are displayed in 33 rows. The child is instructed to mark all figures with four dots, as precise and as fast as they can.(3)

Stroop Color Word Test (Stroop)

The Stroop consists of three trials: in the first trial (Stroop 1) the subject must read color names, in the second trial (Stroop 2) name printed colors, and in the third trial (Stroop 3) name printed colors not denoted by the color name. The test can be administered to children and adults in the age range 8-65 years. Selective attention is measured with this test, using the difference score between Stroop 2 and Stroop 3.(4, 5)

Trail Making Test (TMT)

This paper and pencil test consists of two parts. In the first part (part A), the subject must draw lines to consecutively connect numbered circles on a sheet. In the second part (part B), the subject must consecutively but alternately connect numbered and lettered circles on another worksheet. The aim of the test is to finish each part as quickly as possible. The test can be administered to children and adults in the age range 6-89 years. This test measures visual conceptual and visuomotor tracking as well as divided attention.(4, 5)

Memory

WISC-III-NL – subtest Digit Span

The Digit Span consists of random number sequences that increase in length and that the examiner reads aloud at the rate of 1 number per second. The child has to reproduce these numbers in the same order. Next, the sequences must be recalled backwards (3-5-7 becomes 7-5-3). The first part of the test measures short-term auditory memory and short-term retention capacity. The second part measures auditory working memory.(2)

Wechsler Nonverbal Scale of Ability (WNV) – subtest Spatial Span

The Spatial Span requires the child to touch a group of block arranged on a board in a nonsystematic manner in the same and reverse order as demonstrated by the examiner. The first part of the test measures short-term visuospatial memory and short-term retention capacity. The second part measures visuospatial working-memory.(6)

Rey Auditory Verbal Learning Test (RAVLT)

The RAVLT consists of five presentations with recall of a 15-word list, a sixth recall trial after 30 minutes, and a seventh recognition trial. This test measures memory span, short- and long term verbal memory, verbal recognition, and learning curve. It can be administered to children and adults in the age range 6-89 years.(7, 8)

Memory and visual-spatial functioning

Rey Complex Figure Test (RCFT)

The RCFT consist of three trials. First the child has to copy a complex figure (Copy). Then after 3 and after 30 minutes the figure must be drawn from memory (Recall). Next, different figures are shown and the child has to indicate whether these figures were in the original figure (Recognition). This test measures visual integration, short- and long-term visual-spatial memory, and visual-spatial recognition. It can be completed by children and adults in the age range 6-89 years.(9, 10)

Executive functioning

Key Search

A test of strategy formation. The child is asked to demonstrate how they would search a field for a set of lost keys and their strategy is scored according to its efficiency and functionality.(11)

Modified Six Elements

The child is asked to work on six different tasks for which they have five minutes. The child needs to make sure that by the end of the five minutes, all six of the tasks have been done and the child has done as much as possible of each task. This is a test of planning, task scheduling and performance monitoring.(11)

We used Dutch versions of all tests.

REFERENCES Supplemental Digital Content 1.

1. Kaufman AS, Kaufman JC, Balgopal R, et al. Comparison of three WISC-III short forms: Weighing psychometric, clinical, and practical factors. J Clin Child Psychol 1996;25(1):97-105.
2. Kort W, Compaan EL. WISC NL III. Handleiding: NIP Dienstencentrum 1999.
3. Vos P. Bourdon-Vos. Handleiding (manual dot cancellation test). Lisse: Swets en Zeitlinger; 1992.
4. Lezak MD, Howieson DB, Loring DW. Neuropsychological assessment, 4th ed. Oxford: Oxford University Press; 2004.
5. Schmand B, Houx P, De Koning I. Dutch norms for Stroop color-word test, Trail making test, Rey auditory verbal-learning test, Verbal fluency, and Story recall of Rivermead behavioural memory test. Amsterdam: Division Neuropsychology of the Dutch Institute for Psychology; 2003.
6. Wechsler D, Naglieri JA. Wechsler Nonverbal Scale of Ability San Antonio, TX: Pearson; 2006.
7. van den Burg W, Kingma A. Performance of 225 Dutch school children on Rey's Auditory Verbal Learning Test (AVLT): parallel test-retest reliabilities with an interval of 3 months and normative data. Arch Clin Neuropsychol 1999;14(6):545-559.
8. Schmidt M. Rey Auditory and Verbal Learning Test: a handbook. Los Angeles, CA: Western Psychological Services; 1996.
9. Meyers JE, Meyers, K.R. Rey Complex Figure Test and Recognition Trial Supplemental Norms for Children and Adolescents. Lutz: Psychological Assessment Resources; 1996.
10. Lezak MD, Howieson, D.B., Loring, D.W. Neuropsychological Assessment, 4th ed. . Oxford: Oxford University Express; 2004.
11. Emslie H, Wilson FC, Burden V, et al. Behavioral assessment of the dysexecutive syndrome for children (BADS-C), Dutch version. Amsterdam Harcourt; 2006.

Supplemental Digital Content 2. Neuroimaging methods.

Image Acquisition

Prior to neuroimaging, all participants underwent a 30-minute mock scanning session to become familiarized with the MR-environment[1]. Magnetic resonance imaging data were acquired on a 3 Tesla GE MR-750W system using an 8 channel receive-only head coil (General Electric, Milwaukee, WI). In order to support the participant's head and minimize head motion, cushions were placed on both sides of the child's head inside of the head coil. Participants were able to watch a movie during the scans. MRI-compatible headphones were used to reduce the scanner noise and allow participants to listen to the movie's audio track. Communication with the MR operator was also enabled through the headphones before and after scans. The DTI data were acquired using a single-shot, echo-planar imaging sequence with the following parameters: TR = 12,500 ms, TE = 72 ms, flip angle = 90, matrix = 120 x 120, FOV = 240 mm x 240 mm, slice thickness = 2 mm, number of slices = 65, ASSET acceleration factor = 2. In total, 35 volumes with diffusion weighting (b = 900 s/mm²) and 3 volumes without diffusion weighting (b = 0 s/mm²) were acquired. The high-resolution structural T1-weighted images were acquired using an inversion recovery fast spoiled gradient recalled BRAVO sequence with the following parameters: TR=8.77ms, TE = 3.4ms, inversion time=600ms, flip angel=10, matrix 220x220, FOV=220mm x220mm, ARCimaging acceleration factor of 2, slice thickness = 1mm, and a final $1mm^3$ isotropic resolution.

MR-Image Preprocessing

Data were processed using the Functional MRI of the Brain's Software Library (FMRIB, FSL) (2) and the Camino Diffusion MRI Toolkit within Python (version 2.7) and the Neuroimaging in Python Pipelines and Interfaces package (Nipype, version 0.92)[3,4]. First, motion and eddy-current induced artifacts[5] were addressed using the FSL "eddy_correct" tool[6]. In order to account for the rotations applied to the diffusion data after adjusting for these artifact, the resulting transformation matrices were used to rotate the "B-matrix" gradient direction table[7,8]. The FSL Brain Extraction Tool was used to remove non-brain tissue[9]. In order to minimize the limitations observed with respect to the ordinary least squares fit method[10], the diffusion tensor was fit using the RESTORE method implemented in Camino[11]. Voxel-wise scalar maps (i.e. FA, MD) were then computed. FA is the degree of directionality of diffusion and ranges from 0 to 1, where a higher FA generally represents a greater coherence of white matter fibers. MD is the rate of diffusion of hydrogen averaged in all directions. Lower MD is suggestive of increased integrity in axonal membranes, packing, or myelin. White matter continues to mature throughout childhood, even into young adulthood, causing FA to increase and MD to decrease. Abnormal brain development typically leads to lower FA and higher MD in white matter tracts[12].

Probabilistic Fiber Tractography

Fully automated probabilistic fiber tractography was performed using the FSL plugin, "AutoPtx"[13]. Subject-specific, probabilistic representations of multiple white matter fiber bundles are created with this method using a combination of FSL tools from the Diffusion Toolkit (FDT). The Bayesian Estimation of Diffusion Parameters Obtained using Sampling Techniques (BEDPOSTx), accounting for two fiber orientations at each voxel, was used to esatimate diffusion parameters at each voxel[14,15]. Next, for each subject, the FA map was aligned to the FMRIB-58 FA template image with the FSL nonlinear registration tool (FNIRT). The inverse of this nonlinear warp field was computed, and applied to a series of predefined seed, target, exclusion, and termination masks provided by the AutoPtx plugin (http://fsl.fmrib.ox.ac.uk/fsl/fslwiki/AutoPtx). The FSL module "ProbtrackX" was then applied to conduct probabilistic fiber tracking using these supplied tract-specific masks (i.e., seed, target, etc.) in the native diffusion image space of each subject[14]. The connectivity distributions resulting from fiber tractography were normalized to a scale from 0 to 1 using the total number of successful seed-to-target attempts, and were subsequently thresholded to remove low-probability voxels likely related to noise. For each tract, the number of samples used for probabilistic tracking, and the probability thresholds applied to the resulting distributions (ILF: 0.005, SLF: 0.001, IFO: 0.01, UNC: 0.01, CB: 0.01, PHC: 0.02), were selected based on previously established values[13]. After thresholding the path distributions, weighted average DTI scalar measures were computed within each tract using the normalized path distributions as the weights. The methods used were based on those described by Muetzel et al[16].

Structural Image Acquisition and Analysis

The Freesurfer image analysis suite version 5.3.0 (http://surfer.nmr.mgh.harvard.edu/) for cortical reconstruction and volumetric segmentation was used. Freesurfer computes structural morphometric measures using a fully-automated approach. Technical procedures have been described extensively[19].

Image Quality Assurance

Raw DTI image quality was assessed with both a visual inspection and with automated software[16]. For the visual inspection, maps of the sum of squares error (SSE) of the tensor fit were inspected for structured signal that is consistent with motion and other artifacts in the diffusion-weighted images (e.g., attenuated slices in diffusion-weighted images). Furthermore, probabilistic tractography data were inspected visually to ensure images were properly aligned to the template and paths were reconstructed accurately[16]. Datasets determined to be of poor quality were excluded (n = 7, ~8%).

In addition to this visual inspection, slice-wise signal intensity was examined for attenuation resulting from motion, cardiac pulsation and other artifacts using the automated DTIprep quality control tool (http://www.nitrc.org/projects/dtiprep/). Four (~5%) additional datasets were excluded based on the DTIprep results, leaving 77 DTI datasets (patients = 23, controls = 54) for analysis.

FreeSurfer reconstructions were evaluated for accuracy through detailed visual inspections. Each image was visually inspected and subjects with poor quality data were excluded. In subjects with small errors in the gray/white segmentation, control points, and white matter edits were added to identify and correct misclassified white matter regions. When the segmentation improved, the corrected images were used.

REFERENCES Supplemental Digital Content 2.

1. White T, El Marroun H, Nijs I, Schmidt M, van der Lugt A, Wielopolki PA, et al. Pediatric population-based neuroimaging and the Generation R Study: the intersection of developmental neuroscience and epidemiology. Eur J Epidemiol. 2013;28(1):99-111.
2. Jenkinson M, Beckmann CF, Behrens TE, Woolrich MW, Smith SM. Fsl. Neuroimage. 2012;62(2):782-90.
3. Cook PA, Bai, Y, Nedjati-Gilani, S, Seunarine, KK, Hall, MG, Parker, GJ, Alexander, DC. Camino: open-source diffusion-MRI reconstruction and processing. 14th Scientific Meeting of the International Society for Magnetic Resonance in Medicine. Seattle, WA, USA2006. p. 2759.
4. Gorgolewski K, Burns CD, Madison C, Clark D, Halchenko YO, Waskom ML, et al. Nipype: a flexible, lightweight and extensible neuroimaging data processing framework in python. Front Neuroinform. 2011;5:13.
5. Haselgrove JC, Moore JR. Correction for distortion of echo-planar images used to calculate the apparent diffusion coefficient. Magn Reson Med. 1996;36(6):960-4.
6. Jenkinson M, Smith S. A global optimisation method for robust affine registration of brain images. Med Image Anal. 2001;5(2):143-56.
7. Jones DK, Cercignani M. Twenty-five pitfalls in the analysis of diffusion MRI data. NMR Biomed. 2010;23(7):803-20.
8. Leemans A, Jones DK. The B-matrix must be rotated when correcting for subject motion in DTI data. Magn Reson Med. 2009;61(6):1336-49.
9. Smith SM. Fast robust automated brain extraction. Hum Brain Mapp. 2002;17(3):143-55.
10. Veraart J, Sijbers J, Sunaert S, Leemans A, Jeurissen B. Weighted linear least squares estimation of diffusion MRI parameters: strengths, limitations, and pitfalls. Neuroimage. 2013;81:335-46.
11. Chang LC, Jones DK, Pierpaoli C. RESTORE: robust estimation of tensors by outlier rejection. Magn Reson Med. 2005;53(5):1088-95.
12. Lebel C, Beaulieu C. Longitudinal development of human brain wiring continues from childhood into adulthood. J Neurosci. 2011;31(30):10937-47.
13. de Groot M, Ikram MA, Akoudad S, Krestin GP, Hofman A, van der Lugt A, et al. Tract-specific white matter degeneration in aging: the Rotterdam Study. Alzheimers Dement. 2015;11(3):321-30.
14. Behrens TE, Berg HJ, Jbabdi S, Rushworth MF, Woolrich MW. Probabilistic diffusion tractography with multiple fibre orientations: What can we gain? Neuroimage. 2007;34(1):144-55.
15. Behrens TE, Woolrich MW, Jenkinson M, Johansen-Berg H, Nunes RG, Clare S, et al. Characterization and propagation of uncertainty in diffusion-weighted MR imaging. Magn Reson Med. 2003;50(5):1077-88.
16. Muetzel RL, Mous SE, van der Ende J, Blanken LM, van der Lugt A, Jaddoe VW, et al. White matter integrity and cognitive performance in school-age children: A population-based neuroimaging study. Neuroimage. 2015;119:119-28.
17. Vogt BA, Finch DM, Olson CR. Functional heterogeneity in cingulate cortex: the anterior executive and posterior evaluative regions. Cereb Cortex. 1992;2(6):435-43.
18. van den Bosch GE, H IJsselstijn, van der Lugt A, Tibboel D, van Dijk M, White T. Neuroimaging, Pain Sensitivity, and Neuropsychological Functioning in School-Age Neonatal Extracorporeal Membrane Oxygenation Survivors Exposed to Opioids and Sedatives. Pediatr Crit Care Med. 2015;16(7):652-62.
19. Fischl B, Salat DH, Busa E, et al. Whole brain segmentation: automated labeling of neuroanatomical structures in the human brain. Neuron. 2002; 33:341-355.

Supplemental Digital Content 3. Influence of ECMO treatment and type of ECMO on structure-function relationships.

	DCT	RAVLT delayed recall	RCFT immediate recall	RCFT delayed recall
Global FA	***F*(1,29)=6.74, *p*=.015**			
ECMO treatment	*F*(1,29)=0.23, *p*=.635			
ECMO treatment*GlobalFA	*F*(1,29)=0.23, *p*=.638			
MD left PHC		***F*(1,29)=7.47, *p*=.011**	***F*(1,29)=13.05, *p*<.001**	***F*(1,29)=15.92, *p*<.001**
ECMO treatment		*F*(1,29)=0.00, *p*=.987	*F*(1,29)=0.24, *p*=.629	*F*(1,29)=1.57, *p*=.220
ECMO treatment*MDleftPHC		*F*(1,29)=0.00, *p*=.963	*F*(1,29)=0.27, *p*=.611	*F*(1,29)=1.68, *p*=.205
MD right PHC		***F*(1,29)=9.01, *p*=.005**		
ECMO treatment		*F*(1,29)=0.21, *p*=.647		
ECMO treatment*MDrightPHC		*F*(1,29)=0.29, *p*=.592		
Left hippocampal volume		*F*(1,31)=2.79, *p*=.105		
ECMO treatment		*F*(1,31)=0.05, *p*=.820		
ECMO treatment*LeftHippocampus		*F*(1,31)=0.06, *p*=.829		
Right hippocampal volume		***F*(1,31)=4.39, *p*=.044**		
ECMO treatment		*F*(1,31)=0.45, *p*=.507		
ECMO treatment*RightHippocampus		*F*(1,31)=0.27, *p*=.498		
Global FA	***F*(1,18)=8.05, *p*=.011**			
ECMO type	*F*(1,18)=0.03, *p*=.861			
ECMO type*GlobalFA	*F*(1,18)=0.04, *p*=.837			
MD left PHC		*F*(1,18)=3.60, *p*=.074	***F*(1,18)=8.05, *p*=.011**	*F*(1,18)=4.54, *p*=.047
ECMO type		*F*(1,18)=0.16, *p*=.696	*F*(1,18)=0.15, *p*=.704	*F*(1,18)=0.11, *p*=.738
ECMO type*MDleftPHC		*F*(1,18)=0.17, *p*=.685	*F*(1,18)=0.15, *p*=.700	*F*(1,18)=0.11, *p*=.741
MD right PHC		***F*(1,18)=10.23, *p*=.005**		
ECMO type		*F*(1,18)=0.34, *p*=.565		
ECMO type*MDrightPHC		*F*(1,18)=0.31, *p*=.582		
Left hippocampal volume		***F*(1,20)=5.24, *p*=.033**		
ECMO type		*F*(1,20)=0.61, *p*=.443		
ECMO type*LeftHippocampus		*F*(1,20)=0.61, *p*=.445		
Right hippocampal volume		***F*(1,20)=9.35, *p*=.006**		
ECMO type		*F*(1,20)=0.19, *p*=.665		
ECMO type*RightHippocampus		*F*(1,20)=0.27, *p*=.608		

Results of linear regression analsyes assessing differences between patients treated with ECMO and without ECMO in the significant structure-function relationships. The same analyses were conducted to assess differences between patients treated with venoarterial and venovenous ECMO (ECMOtype). ***P*** < .05 is considered statistically significant.

Abbreviations: FA, fractional anisotropy; MD, mean diffusivity; PHC, parahippocampal region of the cingulum; DCT, Dot Cancellation Test; RAVLT, Rey Auditory Verbal Learning Test; RCFT, Rey Complex Figure Test.